

Motion Planning and Model Predictive Control for Automated Tractor-Trailer Hitching Maneuver

Wang, Zejiang; Ahmad, Ahmad; Quirynen, Rien; Wang, Yebin; Bhagat, Akshay; Zeino, Eyad;
Zushi, Yuji; Di Cairano, Stefano

TR2022-109 September 29, 2022

Abstract

In recent years significant progress has been made in optimization-based planning and control for automated vehicle operation. For heavy-duty vehicles, the research focus has been on platooning and control of articulated vehicles especially when cruising on the highway. This paper proposes an integrated system using a motion planning algorithm and a real-time reference tracking controller, tailored to the task of automated tractor-trailer hitching which is a critical maneuver in heavy-duty vehicle operations, due to requiring a very high precision. The motion planner is based on a bi-directional A- search guided tree algorithm and the tracking controller is implemented using nonlinear model predictive control. To validate the proposed approach, we present results from hardware-in-the-loop simulations on a dSPACE Scalexio real-time computing unit and extensive Monte Carlo closed-loop simulations.

IEEE Conference on Control Technology and Applications (CCTA) 2022

Motion Planning and Model Predictive Control for Automated Tractor-Trailer Hitching Maneuver

Zejiang Wang^{1,3}, Ahmad Ahmad^{1,4}, Rien Quirynen¹, Yebin Wang¹,
Akshay Bhagat², Eyad Zeino², Yuji Zushi², and Stefano Di Cairano¹

Abstract—In recent years significant progress has been made in optimization-based planning and control for automated vehicle operation. For heavy-duty vehicles, the research focus has been on platooning and control of articulated vehicles especially when cruising on the highway. This paper proposes an integrated system using a motion planning algorithm and a real-time reference tracking controller, tailored to the task of automated tractor-trailer hitching which is a critical maneuver in heavy-duty vehicle operations, due to requiring a very high precision. The motion planner is based on a bi-directional A-search guided tree algorithm and the tracking controller is implemented using nonlinear model predictive control. To validate the proposed approach, we present results from hardware-in-the-loop simulations on a dSPACE Scalexio real-time computing unit and extensive Monte Carlo closed-loop simulations.

I. INTRODUCTION

Automated transportation systems, even in the case of partial automation, can lead to reduced accidents and more efficient usage of the vehicles and infrastructure. Connected and automated vehicles (CAVs) show large promises for improving safety and traffic flow, and as a consequence for reducing congestion, travel time, emissions and energy consumption [1], [2]. Commercial heavy-duty vehicles (HDV) such as trucks are an important use case of vehicle automation, as trucks cover a higher mileage, in average about 100,000 km/year, compared to passenger vehicles, in average 14,000 km/year [3]. In particular, considering the increasingly high complexity of supply chain management [4], automated trucks can provide considerable advantages with respect to economic, environmental, and social factors [3].

Optimization-based motion planning and control techniques have been investigated for automation of HDVs different tasks, such as platooning during highway driving [5]. A different and challenging maneuver for HDVs, which requires extensive and expensive labor training, is tractor-trailer hitching. During the hitching maneuver, the driver needs to accurately control the position and orientation of a truck while executing a sequence of forward and reverse motions to connect the truck with a trailer standing still, see Fig. 1. During the process, the driver may have a limited vision of the area around the target hitching point.

¹Mitsubishi Electric Research Laboratories, Cambridge, MA, USA {quirynen,yebinwang,dicairano}@merl.com.

²Mitsubishi Electric Automotive America, Northville, MI, USA {ABhagat,EZeino,YZushi}@meaa.mea.com.

³The University of Texas at Austin, Austin, TX, USA wangzejiang@utexas.edu.

⁴Boston University, Boston, MA, USA ahmadgh@bu.edu.

Most prior works focus on articulated tractor-trailer operation, while ignoring the hitching maneuver that may seem easier but requires a comparably higher precision and is a key task in HDV operation. In regards to tractor-trailer motion planning, different techniques have been proposed, such as sampling-based, lattice-based or combined algorithms [6]–[8]. Different control algorithms have been proposed to track the resulting motion plan for a tractor-trailer system, e.g., sliding mode control [9], input-state linearization [10], and model predictive control [11].

Instead, the present paper proposes an integrated system using a tree-based motion planning algorithm and a real-time reference tracking controller, tailored to the task of automated tractor-trailer hitching. In particular, we present a modified variant of the bi-directional A-search guided tree (BIAGT) path and motion planning algorithm that was originally proposed in [12]. For tracking the obtained reference trajectory from the BIAGT algorithm so to successfully complete the hitching maneuver, we develop a real-time feasible implementation of a nonlinear model predictive controller (NMPC) for the combined lateral and longitudinal dynamics of the tractor. The contributions of this work include: (i) tailored modifications of the BIAGT algorithm for motion planning of the tractor-trailer hitching maneuver; (ii) an NMPC design for reference tracking that is offset-free to meet the stringent precision requirements of the hitching maneuver; (iii) a software implementation of the integrated system that is real-time feasible on a dSPACE Scalexio unit; (iv) hardware-in-the-loop (HIL) validation results of planner and controller for automated tractor-trailer hitching.

The rest of the paper is organized as follows. Section II describes the problem statement, Section III presents the BIAGT motion planner, and Section IV describes the NMPC. Section V discusses the tailored integration of the planning and control algorithms, and Section VI presents the HIL validation results. Finally, Section VII concludes this paper.

II. PROBLEM STATEMENT AND MOTIVATION

The tractor-trailer hitching maneuver investigated in this work is illustrated in Fig. 1. The truck tractor, hereafter often referred to simply as “truck”, maneuvers in forward and reverse consecutively while steering towards the hitching point, where the tractor’s hitching mechanism, the so-called “fifth wheel”, connects to the trailer standing still. Unlike typical automated driving on highways or urban environments, the hitching maneuver is more lenient to the path tracking errors when the tractor is far from the hitching point,

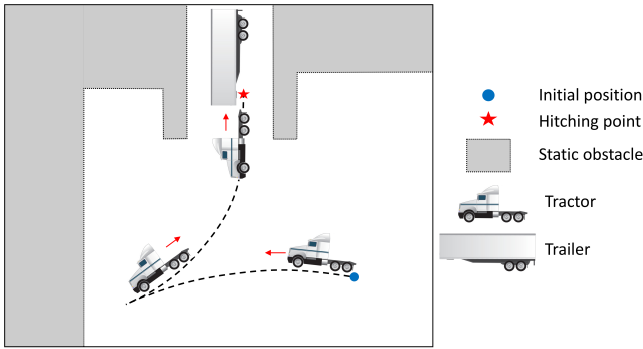


Fig. 1. Illustration of a tractor-trailer hitching maneuver.

but is very stringent in both lateral position and heading error requirements in a neighborhood of the hitching point, in order not to damage the hitching mechanism and to successfully connect to the trailer. The requirements for the automated hitching system are as follows.

Problem 1 (Automated Tractor-Trailer Hitching): Let the set of tractor poses be defined as $\mathcal{P} \subset \mathbb{R}^3$ and $\mathcal{P}_{\text{free}} \subset \mathcal{P}$ denotes the set of collision-free poses. Starting from an initial pose $p_0 \in \mathcal{P}_{\text{free}}$ with zero velocity, and given a hitching pose $p_f \in \mathcal{P}_{\text{free}}$, the proposed system computes a trajectory and controls the tractor (or truck) to execute a maneuver that meets the following requirements:

- 1) the vehicle operation during hitching maneuver is automated without human intervention;
- 2) a kinematically feasible reference trajectory is computed online, starting from p_0 and ending in p_f , while avoiding collisions between the tractor and any static obstacles in the environment;
- 3) for successful hitching and for the safety of the hitching mechanism, a lateral position error $|e_Y| < 0.1$ m and a heading error $|e_\psi| < 10$ deg with respect to the preferred hitching orientation, is required, in a set $\mathcal{P}_f \subset \mathcal{P}_{\text{free}}$ around the hitching pose $p_f \in \mathcal{P}_f$;
- 4) if a dynamic obstacle enters a safety region around the current or predicted tractor positions, trajectory tracking is interrupted by an emergency braking system, and tracking is resumed after the obstacle moves away.

In addition, the planning and control algorithms need to run on an automotive grade embedded system platform and meet the real-time requirements:

- 1) motion planning is executed once at standstill, and computed within a maximum time of 2 – 5 seconds;
- 2) trajectory tracking is executed continuously while the tractor is moving with sampling time of $T_s = 50$ ms.

A. Vehicle Kinematic Model

Under the assumption of normal driving conditions, i.e., not at-the-limit maneuvers, we use a single-track vehicle model in which the two wheels on each axle are lumped together. If the tractor is equipped with multiple rear axes, see Fig. 1 for an example, those are lumped together resulting in a model with only two wheels, one at the front and one

at the rear. Summarizing, we use the kinematic single-track vehicle model

$$\begin{aligned} \dot{p}_X &= v \cos(\psi), & \dot{p}_Y &= v \sin(\psi), \\ \dot{\psi} &= v \tan(\delta_f) / L, & \dot{\delta}_f &= (\delta - \delta_f) / \tau, \end{aligned} \quad (1)$$

where $(p_X, p_Y, \psi) \in \mathcal{P}$ denotes the tractor's pose, p_X, p_Y is the longitudinal-lateral position, ψ is the heading angle and $\dot{\psi}$ the heading rate, v is the longitudinal velocity of the tractor, δ and δ_f are the commanded and actual front wheel steering angle, respectively, L is the wheel base of the tractor and τ is the time constant of the steering actuator.

We further assume that the current state of the vehicle is estimated by on-board sensor fusion, and the errors are sufficiently small to be compensated by the feedback controller (see results in Section VI). Obstacles in the environment can be detected by on-board sensors or using communication with sensing infrastructure as described in [13].

III. PATH AND MOTION PLANNING FOR TRACTOR-TRAILER HITCHING MANEUVER

This section describes the bi-directional A-search guided tree (BIAGT) path and motion planning algorithm initially presented in [12]. BIAGT can efficiently compute kinematically feasible solutions for automated vehicle parking tasks. The tractor-trailer hitching maneuver described in Problem 1 may be considered a special parking task with very stringent requirements on the terminal phase of the maneuver in terms of lateral position and heading angle errors.

A. Bi-Directional A-Search Guided Tree (BIAGT)

BIAGT improves the hybrid A* algorithm [14] in two aspects. Given the configuration space \mathcal{P} of truck poses, including position and heading, first, it prioritizes the control actions at each node to balance optimality of the computed path and computational efficiency. Second, it simultaneously expands two trees, i.e., the start tree from the starting configuration of the tractor and the goal tree from the hitching point configuration at the trailer. Particularly, one tree leverages the arrival cost of the other tree to estimate the cost-to-go of its own nodes. An implementation of the BIAGT planner is described in Algorithm 1 and more details can be found in [12]. Once a feasible path is found, BIAGT executes a motion planning step to determine the velocity profile along the path, and outputs a motion plan.

We define a tree $\mathcal{T} = (\mathcal{V}, \mathcal{E})$ as a union of a node set $\mathcal{V} \subset \mathcal{P}_{\text{free}}$ and an edge set \mathcal{E} , where $E(X_i, X_j) \in \mathcal{E}$ is a feasible, collision-free, trajectory between state values X_i and X_j and $\mathcal{P}_{\text{free}}$ is implicitly obtained by checking collisions with static obstacles in the environment, see Fig. 1. Let \mathcal{M} denote a finite set of motion primitives precomputed from the available control actions, and V_{max} the allowed maximum number of nodes. BIAGT constructs a start tree \mathcal{T}_s rooted at X_0 (Line 13 in Alg. 1) and a goal tree \mathcal{T}_g rooted at X_f (Line 16), and it expands each tree according to a cost function $F(\cdot)$ that sums a heuristic value $h(\cdot)$ and arrival cost $g(\cdot)$. The heuristics in BIAGT are calculated based on the Reeds-Shepp (RS) path length [15] towards

Algorithm 1: BIAGT Path and Motion Planning

```
1 input  $\mathcal{P}_{\text{free}}, X_0, X_f, V_{\text{max}}, \mathcal{M}, \epsilon$ 
2  $\mathcal{T}_s \leftarrow (X_0, \emptyset), \mathcal{T}_g \leftarrow (X_f, \emptyset)$ 
3  $F(X_0) \leftarrow g(X_0) + h(X_0), F(X_f) \leftarrow g(X_f) + h(X_f)$ 
4  $Q_s \leftarrow (X_0, F(X_0)), Q_g \leftarrow (X_f, F(X_f))$ 
5  $k \leftarrow 2, \text{success} \leftarrow \text{false}$ 
6 while  $k \leq V_{\text{max}}$  and not success do
7    $X_{\text{best}}^s = Q_s.\text{Pop}$  where  $F(X_{\text{best}}^s) \leq F(X), \forall X \in Q_s$ 
8    $X_{\text{best}}^g = Q_g.\text{Pop}$  where  $F(X_{\text{best}}^g) \leq F(X), \forall X \in Q_g$ 
9   if  $d(X_{\text{best}}^s, X_f) \leq \epsilon$  or  $d(X_{\text{best}}^g, X_0) \leq \epsilon$  then
10     $\text{success} \leftarrow \text{true}$ 
11  else if  $\text{dist}(\mathcal{T}_s, \mathcal{T}_g) \leq \epsilon$  then  $\text{Connect}(\mathcal{T}_s, \mathcal{T}_g)$ ;
12  else
13     $(\text{success}, n_s) \leftarrow \text{Expand}(\mathcal{T}_s, \mathcal{P}_{\text{free}}, X_{\text{best}}^s, \mathcal{M})$ 
14    Compute  $F$  for new nodes and append to  $Q_s$ 
15    if not success then
16       $(\text{success}, n_g) \leftarrow \text{Expand}(\mathcal{T}_g, \mathcal{P}_{\text{free}}, X_{\text{best}}^g, \mathcal{M})$ 
17      Compute  $F$  for new nodes and append to  $Q_g$ 
18     $k \leftarrow k + n_s + n_g$ 
19 return  $\mathcal{T}_{\text{plan}} = \text{FeasiblePath}(\mathcal{T}_s, \mathcal{T}_g, \text{success})$ 
```

the tree corresponding goal while ignoring the obstacles. If either tree gets close to the corresponding goal or the distance between the two trees is smaller than or equal to a threshold ϵ , then BIAGT will connect the two trees with a dynamically feasible path according to model (1). If the connection succeeds (Line 11), all parents of the connected nodes are added to the other tree resulting in a feasible path, thus planning is successful. If the total number of nodes on both trees reaches V_{max} and a solution trajectory has not yet been found, planning fails.

B. BIAGT Adaptation to Tractor-Trailer Hitching Maneuver

To further enhance the performance of the BIAGT algorithm for path and motion planning in the proposed automated tractor-trailer hitching system, and to improve the performance of the NMPC controller that is described in the next section for tracking the resulting reference trajectory, we propose the following tailored modifications.

First, instead of starting the goal tree exactly from the hitching point, we place the root of the goal tree a user-defined distance of, e.g., 10 m away from the hitching point, in the preferred hitching direction away from the trailer, and we connect the hitching point and this actual goal tree root with a straight line. This ensures that the BIAGT computes a motion plan that ends with a straight line segment before the tractor is arriving in the neighborhood of the hitching point, in order not to damage the hitching mechanism and to meet the strict requirements as described in Problem 1.

Second, the path quality, such as the number of motion cusps, can be an important factor for accuracy of the tractor-trailer hitching maneuver. Thus, we customize the BIAGT to search for a path with a minimum number of motion cusps. Various options can be attempted to achieve this behavior, e.g., by penalizing the change of velocity direction in the arrival cost. In order to balance the completeness, computational efficiency, and path quality, we propose the

following two-step process. The first step ensures feasibility by executing the original BIAGT to find a path as quick as possible. The second step improves path quality by imposing the desired maximum amount of motion cusps as a hard constraint during the node selection. Particularly, for any node in the priority queue, if the segment between the node and the root node of the corresponding tree contains more motion cusps than the allowed amount, the node will be removed from the queue without further expansion. The path quality improvement step keeps running until either the planner times out or such a desirable path is found.

Finally, since BIAGT computes a motion plan for tractor-trailer hitching that typically includes one or multiple motion cusps, i.e., switches between forward and backward tractor driving direction. For this purpose, the generated motion trajectories include a pause, e.g., of 2 s at each motion cusp. This allows to accommodate the physical time for gear shifting, as it will be discussed later and also improves the tracking performance when a predictive controller is used.

IV. NONLINEAR MODEL PREDICTIVE CONTROL FOR TRAJECTORY TRACKING

Next, we design the nonlinear model predictive controller (NMPC) for accurately tracking the planned trajectory $(p_X^{\text{ref}}(t_i), p_Y^{\text{ref}}(t_i), \psi^{\text{ref}}(t_i), v^{\text{ref}}(t_i))_{i=0, \dots, M}$, given a grid of time points $t_0 < t_1 < \dots < t_i < \dots < t_M$ over the planning horizon for the tractor-trailer hitching maneuver.

A. Extended Vehicle Kinematics Model

First, we augment the vehicle model (1) by including the acceleration a and rate of change δ_{rate} for the commanded front wheel steering angle

$$\dot{v} = a, \quad \dot{\delta} = \delta_{\text{rate}}. \quad (2)$$

Even though the vehicle speed, v , and front wheel steering angle, δ , are control commands that are typically sent to a low-level control-by-wire system, Eq. (2) enables introducing the acceleration and steering angle rate of change in the objective function and constraints of the NMPC problem.

We model the lateral position error with respect to the planned reference trajectory by

$$e_Y = \cos(\psi^{\text{ref}}) (p_Y - p_Y^{\text{ref}}) - \sin(\psi^{\text{ref}}) (p_X - p_X^{\text{ref}}). \quad (3)$$

To achieve an offset-free design [16], we add integral action to the NMPC formulation by including in the vehicle model the error integrator $\dot{e}_Y^{\text{int}} = e_Y$.

The resulting augmented vehicle prediction model is

$$\begin{aligned} \dot{p}_X &= v \cos(\psi), & \dot{p}_Y &= v \sin(\psi), \\ \dot{\psi} &= v \tan(\delta_f) / L, & \dot{\delta}_f &= (\delta - \delta_f) / \tau, \\ \dot{v} &= a, & \dot{\delta} &= \delta_{\text{rate}}, \\ \dot{e}_Y^{\text{int}} &= \cos(\psi^{\text{ref}}) (p_Y - p_Y^{\text{ref}}) - \sin(\psi^{\text{ref}}) (p_X - p_X^{\text{ref}}), \end{aligned} \quad (4)$$

with $n_x = 7$ states, $x = [p_X \ p_Y \ \psi \ \delta_f \ v \ \delta \ e_Y^{\text{int}}]^\top$, and $n_u = 2$ control inputs, $u = [a \ \delta_{\text{rate}}]^\top$.

B. Direct Multiple Shooting Discretization

The NMPC minimizes the vehicle's tracking errors with respect to the planned reference trajectory $(p_X^{\text{ref}}(t_i), p_Y^{\text{ref}}(t_i), \psi^{\text{ref}}(t_i), v^{\text{ref}}(t_i))_{i=0, \dots, M}$, while satisfying constraints on longitudinal speed, acceleration, front wheel steering angle and its change rate. We formulate the constrained optimal control problem (OCP) using direct multiple shooting. At each control time step t_i , based on a time grid of equidistant time points t_k for $k = 0, \dots, N$, $t_{k+1} - t_k = \frac{T}{N}$, where T is the horizon length and N is the number of control intervals, we apply a piecewise constant control parameterization $u(t_i + \tau|t_i) = u_{i,k}$ for $\tau \in [t_k, t_{k+1})$, where $u_{i,k}$ is the predicted control input for $\tau \in [t_k, t_{k+1})$, computed at time step t_i . For simplicity, the equidistant time grid is aligned with the discrete time points of the planned reference trajectory, $x_{i,k}^{\text{ref}} = x^{\text{ref}}(t_i + t_k)$. Alternatively, a polynomial interpolation could be used.

Given a state estimate $\hat{x}_{i,0}$ at time step t_i and the piecewise constant control parameterization, we discretize the dynamics in (4) by a numerical integration method, resulting in the discrete-time prediction model

$$x_{i,k+1} = f(x_{i,k}, u_{i,k}), \quad k = 0, \dots, N-1. \quad (5)$$

We apply the explicit 4th order Runge-Kutta method, but also other integration schemes can achieve the desired accuracy.

C. Constrained Optimal Control Problem Formulation

The NMPC cost function is based on the least squares tracking formulation

$$J(X_i, U_i, S_i) = \frac{1}{2} \sum_{k=0}^{N-1} \left(\|x_{i,k} - x_{i,k}^{\text{ref}}\|_Q^2 + \|u_{i,k}\|_R^2 \right) \quad (6a)$$

$$+ \frac{1}{2} \|x_{i,N} - x_{i,N}^{\text{ref}}\|_P^2 + \sum_{k=0}^N \rho s_{i,k}, \quad (6b)$$

where $Q \succeq 0$, $P \succeq 0$ are positive semi-definite, $R > 0$ is positive definite, the reference state vector is $x^{\text{ref}} = [p_X^{\text{ref}}, p_Y^{\text{ref}}, \psi^{\text{ref}}, 0, v^{\text{ref}}, 0, 0]$, and $s_{i,k}$ are non-negative slack variables that soften the constraints to ensure recursive feasibility, and are penalized in a linear term in (6b). We denote $X_i = [x_{i,0}^\top, \dots, x_{i,N}^\top]^\top$, $U_i = [u_{i,0}^\top, \dots, u_{i,N-1}^\top]^\top$ and slack variables $S_i = [s_{i,0}^\top, \dots, s_{i,N}^\top]^\top$.

Given the cost function (6), we formulate the OCP

$$\min_{X_i, U_i, S_i} J(X_i, U_i, S_i) \quad (7a)$$

$$\text{s.t. } x_{i,0} = \hat{x}_{i,0}, \quad (7b)$$

$$x_{i,k+1} = f(x_{i,k}, u_{i,k}), \quad \forall k \in \mathbb{Z}_0^{N-1}, \quad (7c)$$

$$-\delta_f^{\max} - s_{i,k} \leq \delta_{f_i,k} \leq \delta_f^{\max} + s_{i,k}, \quad \forall k \in \mathbb{Z}_0^N, \quad (7d)$$

$$v^{\min} - s_{i,k} \leq v_{i,k} \leq v^{\max} + s_{i,k}, \quad \forall k \in \mathbb{Z}_0^N, \quad (7e)$$

$$-\delta^{\max} \leq \delta_{i,k} \leq \delta^{\max}, \quad \forall k \in \mathbb{Z}_0^N, \quad (7f)$$

$$a^{\min} \leq a_{i,k} \leq a^{\max}, \quad \forall k \in \mathbb{Z}_0^{N-1}, \quad (7g)$$

$$-\delta_{\text{rate}}^{\max} \leq \delta_{\text{rate},i,k} \leq \delta_{\text{rate}}^{\max}, \quad \forall k \in \mathbb{Z}_0^{N-1}, \quad (7h)$$

$$0 \leq s_{i,k}, \quad \forall k \in \mathbb{Z}_0^N, \quad (7i)$$

where \mathbb{Z}_a^b denotes the range of integers $a, a+1, \dots, b$, eqs. (7d)-(7i) impose inequality constraints on the steering angle, velocity, steering command, acceleration, steering rate and on the slack variable, respectively. A sufficiently large weight value $\rho > 0$ in the cost function (6) ensures that $s_{i,k} = 0$, $k \in \mathbb{Z}_0^N$ whenever the constraints can be satisfied.

Remark 1: The quadratic penalty on the integrated error e_Y^{int} in (6) determines how offset-free tracking control $e_Y \rightarrow 0$ is achieved, to meet hitching requirements at the end of the maneuver. To avoid oscillations, the integrated error e_Y^{int} can be reset whenever its value grows too large or when the lateral position error e_Y is sufficiently close to zero.

D. Real-time NMPC Implementation

We implement the NMPC with a sampling period of $T_s = \frac{T}{N} = 50$ ms. At each control time step t_i , given the current velocity $\hat{v}_{i,0}$ and steering angle $\hat{\delta}_{i,0}$, we compute the velocity and steering commands for the control-by-wire system from the solution U_i^* of the optimal control problem (7),

$$v_{\text{MPC}}(t_i) = \hat{v}_{i,0} + T_s a_{i,0}^*, \quad \delta_{\text{MPC}}(t_i) = \hat{\delta}_{i,0} + T_s \delta_{\text{rate},i,0}^*. \quad (8)$$

In case of a time delay, e.g., due to the vehicle network communication and/or actuator interface, a prediction-based time delay compensation can be used [17].

We solve the nonlinear program in (7) within the sampling time of $T_s = 50$ ms by a tailored implementation of sequential quadratic programming (SQP) known as the real-time iterations (RTI) scheme [18]. The RTI algorithm performs a single SQP iteration per control time step, and uses a continuation-based warm starting of the state and control trajectories (X_i, U_i, S_i) from one time step t_i to the next t_{i+1} . The nonlinear functions and their first order derivatives are evaluated efficiently using C code generation in CasADi [19]. We use the QP solver PRESAS [20], which applies block-structured factorization techniques with low-rank updates to preconditioning of an iterative solver within a primal active-set algorithm. In combination with the CasADi generated C code, this results in an efficient NMPC solver that is suitable for embedded system platforms.

V. INTEGRATED SYSTEM FOR AUTOMATED TRACTOR-TRAILER HITCHING

Next, we discuss the integration of the BIAGT motion planning algorithm from Section III and the NMPC tracking controller from Section IV for tractor-trailer hitching.

A. Automatic Emergency Braking (AEB)

As stated in Problem 1, the BIAGT motion planning algorithm computes a kinematically feasible trajectory that avoids collisions between the tractor and any static obstacles in the environment. Regarding other dynamic obstacles, we make the following assumptions:

- The tractor-trailer hitching maneuver is carried out in a mostly closed environment, i.e., without pedestrians, cyclists, or passenger vehicles, and with only sporadic appearances of dynamic obstacles in the area of interest.

- If a dynamic obstacle appears while performing the hitching maneuver, the system stops by performing an automatic emergency braking (AEB), and resumes execution of the maneuver after the dynamic obstacle has moved outside of a predefined safety region.

AEB is initiated if a dynamic obstacle is detected, using on-board sensors or by communication, and if the obstacle is within the union of safety regions around the current or predicted positions of the truck. While AEB is engaged, the NMPC tracking controller is interrupted and a braking maneuver is executed. When the obstacle moves outside the union of safety regions, the NMPC tracking controller is re-initialized and the automated hitching maneuver continues.

In most cases, due to the low speeds at which the tractor executes the hitching maneuver, the same motion plan can be reused to complete the maneuver and the BIAGT algorithm does not need to be executed after such an interruption. The proposed method can be extended to include fast re-planning of the motion plan [21] and obstacle avoidance constraints in the NMPC problem formulation [22].

B. Motion Planning and NMPC for Gear Shifting

As mentioned in Section III, the BIAGT motion planning algorithm is modified to introduce a pause at each cusp, i.e., at each switch between forward and backward motion of the truck to reach the hitching point at the end of the maneuver. In the pause period Δt_{pause} , during which the tractor is planned to be at standstill, a gear shift is initiated with a preview Δt_{pre} before the tractor starts moving in the opposite direction. The preview period is chosen to be larger than the average time it takes for the tractor to switch between gears, $\Delta t_{\text{pre}} > \Delta t_{\text{gear}}$. The longitudinal velocity bounds in (7e), v^{\min} , v^{\max} , change according to the current gear, $v \geq 0$ when the tractor is in *Drive*, and $v \leq 0$ when it is in *Reverse*.

VI. CLOSED-LOOP SIMULATIONS AND HIL VALIDATION

We validate the performance of the automated tractor-trailer hitching system, consisting of motion planner and tracking controller, based on closed-loop Matlab simulations and HIL validations on a dSPACE Scalexio unit. The parameter values are based on a real truck. For the NMPC controller, in (6) we use the parameters: $T_s = 0.05$ s, $N = 40$, $Q = \text{diag}([1, 1, 1, 10^{-4}, 10^{-1}, 10^{-4}, 10^{-2}])$, $R = \text{diag}([10^{-2}, 10^{-3}])$, and $\rho = 10$. The bounds in (7) are $\delta_f^{\max} = \delta^{\max} = 36$ deg, $\delta_{\text{rate}}^{\max} = 30$ deg/s, $a^{\max} = 1$ m/s², $a^{\min} = -4$ m/s². The speed limits are $v^{\min} = 0$ m/s and $v^{\max} = 2$ m/s if the gear is *Drive*, or $v^{\min} = -2$ m/s and $v^{\max} = 0$ m/s if the gear is *Reverse*.

A. Vehicle Model Mismatch and Sensor Noise Levels

The closed-loop simulations are executed with the vehicle kinematics model in (1). Therefore, the system states include p_X , p_Y , ψ and δ_f , and the control inputs are v and δ and they are provided directly by the NMPC controller as in Eq. (8). The NMPC model in (4) uses the nominal parameter values

$L_0 = 5.52$ m and $\tau_0 = 0.2$ s. However, to validate robustness of the proposed integrated automated hitching system, an unknown mismatch is included between the simulation model and the NMPC prediction model. Specifically, the parameter values for the simulation model are chosen to be $L = L_0 + 0.1$ m and $\tau = \tau_0 + 0.1$ s. In addition, we include a constant offset for the front wheel steering angle, i.e.,

$$\dot{\delta}_f = (\delta + \delta_{\text{offset}} - \delta_f) / \tau, \quad (9)$$

where the offset value $\delta_{\text{offset}} = 1$ deg. The state vector, which provides the initial value $\hat{x}_{i,0}$ to NMPC problem at each time step t_i , is measured, and we add sensor noise as a zero-mean Gaussian random vector with covariance matrix $\text{diag}([4.5, 4.5, 18, 4.5] \times 10^{-5})$.

B. Closed-loop Performance of Automated Hitching System

Fig. 2 shows closed-loop simulations of the tractor-trailer hitching maneuver using the BIAGT motion planner and the NMPC tracking controller for a fixed hitching point at the trailer and three different initial tractor positions, resulting in paths with one (red), two (purple), and three (green) motion cusps. The dashed lines are the planned path and the dotted lines are the closed-loop simulated trajectories using NMPC. The bottom three plots in Fig. 2 show the error values between planned and simulated trajectories for the lateral position, heading angle and velocity, respectively.

Fig. 2 shows that the BIAGT algorithm may compute a motion plan with a different number of motion cusps, depending on the initial starting point of the tractor. Fig. 2 also shows that, for each of the three initial conditions, the terminal position and heading errors with respect to the hitching point are within the requirements in Problem 1, i.e., $|e_Y| < 0.1$ m and $|e_\psi| < 10$ deg. The BIAGT's motion plan straight segment near the hitching point helps the NMPC integral action in achieving a closed-loop trajectory that converges to the reference trajectory.

The behavior of the motion planner and tracking controller with gear shifts is illustrated in Fig. 3. The gear positions 4 and 2 correspond to the *Drive* and *Reverse*, respectively. Fig. 3 shows the two cases when there is no dynamic obstacle, and when a dynamic obstacle is detected around $t = 55$ s so that the AEB system is activated. In both cases, the gear shifts from *Drive* to the *Reverse* before the tractor is expected to start driving backwards, as required.

C. Real-time Validation on dSPACE Scalexio

The HIL simulations are executed on a dSPACE Scalexio DS6001 computing unit. To guarantee real-time execution, the NMPC turnaround time (TAT) must be less than the sampling period $T_s = 50$ ms. As shown in Fig. 4, the TATs for the NMPC tracking controller are typically below 10 ms, well below 50 ms. Fig. 4 also shows the TATs for the BIAGT motion planner, which is executed only once at the beginning of the automated tractor-trailer hitching maneuver, as per the specifications in Problem 1. After the reference trajectory is computed, which takes less than 1 s in Fig. 4, the NMPC tracking controller is activated to accurately steer the tractor

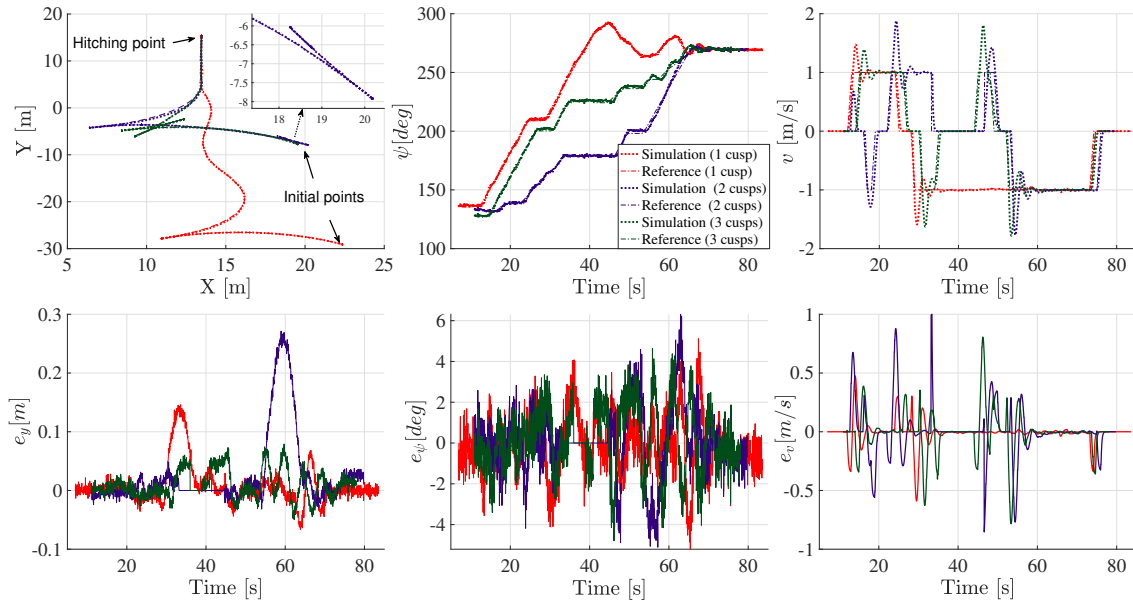


Fig. 2. Closed-loop simulation results from the BIAGT motion planner and NMPC tracking controller, for a fixed hitching point and three different initial positions of the tractor, resulting in paths with one (red), two (purple), or three (green) cusps to complete the hitching maneuver.

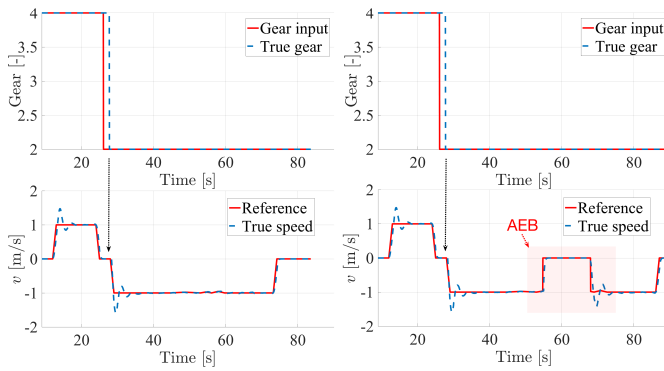


Fig. 3. Reference and achieved tractor velocity with gear shift commands and gear shift delays, without (left) and with (right) a dynamic obstacle, causing temporary AEB activation for safety.

along the motion plan. The BIAGT algorithm requires a computational effort only at the first time step to compute the reference. However, TATs for the planner in Fig. 4 are nonzero at all time steps, because the NMPC and BIAGT algorithms are executed on a single core of the dSPACE Scalexio unit and the NMPC task has the highest priority.

D. Monte Carlo Simulations with Random Initial Conditions

As shown in Fig. 2, the BIAGT planner may compute a motion plan with a different number of motion cusps, depending on the initial pose of the tractor. Therefore, we execute Monte Carlo simulations in Matlab with randomized initial positions and heading angles. We randomly sample 2000 initial conditions from the state space region defined by $14 \leq p_X \leq 28$ m, $-17 \leq p_Y \leq -1$ m, and $115 \leq \psi \leq 172$ deg. The performance of the BIAGT motion planner for the 2000 simulations is summarized as shown in Fig. 5.

Fig. 5 shows that for all the 2000 cases, the BIAGT

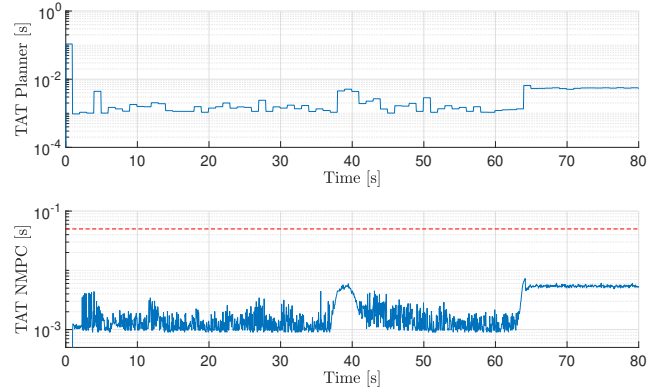


Fig. 4. Turnaround times (TATs) for the BIAGT and the NMPC tasks in the dSPACE Scalexio real-time computing unit.

motion planner can always compute a feasible trajectory, from the initial condition to the hitching point. As discussed in Section V, reducing the number of motion cusps in the motion plan usually improves the tracking performance. In the 2000 simulations, 76%, 9% and 15% of the plans have 1, 2 and 3 motion cusps, respectively. Fig. 5 also shows the time to compute the motion plan in the Monte Carlo simulations, which shows that BIAGT can compute the motion plan within 1 s for 79% of the cases. As discussed in Section III, the tailored BIAGT algorithm aims to reduce the number of motion cusps in the plan, after a trajectory with a larger number of motion cusps has already been found. Therefore, even though the motion planner reached the maximum time limit of 5 s in 15% of the cases, a motion plan with 3 motion cusps was already found earlier.

Fig. 6 summarizes the closed-loop NMPC performance in the 2000 Monte Carlo simulations, in terms of position

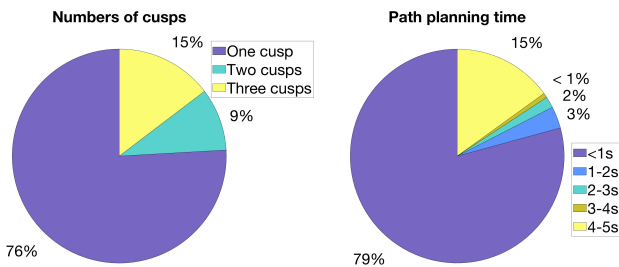


Fig. 5. BIAGT planner performance results for 2000 Monte Carlo simulations: number of motion cusps (left) and computation time (right).

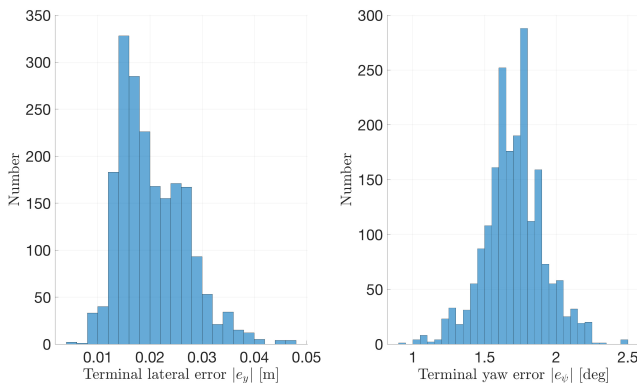


Fig. 6. Terminal position and heading angle errors of NMPC for the automated hitching maneuver in 2000 closed-loop Monte Carlo simulations.

and heading angle error at the terminal point of the automated tractor-trailer hitching maneuver. The histograms of the terminal errors in Fig. 6 confirm that the specifications of Problem 1, $|e_Y| < 0.1$ m and $|e_\psi| < 10$ deg are satisfied in all the 2000 simulation scenarios.

VII. CONCLUSIONS

We have proposed a system for integrated motion planning and control for automated tractor-trailer hitching. The BIAGT planner yields a kinematically feasible and safe trajectory from the initial point to the hitching point. An NMPC accurately tracks the reference path while satisfying the system constraints. Safety with respect to dynamic obstacles is provided by an automatic emergency braking system, and gear shifting is taken into account. Hardware-in-the-loop simulations on a dSPACE Scalexio unit demonstrate the feasibility and effectiveness of the planning and control system. The requirements on the lateral position and heading angle errors with respect to the hitching point are satisfied. Validation of the proposed framework in real tractor-trailer hitching experiments is ongoing.

REFERENCES

- [1] J. Guanetti, Y. Kim, and F. Borrelli, “Control of connected and automated vehicles: State of the art and future challenges,” *Annual Reviews in Control*, vol. 45, pp. 18 – 40, 2018.
- [2] T. Ersal, I. Kolmanovsky, N. Masoud, N. Ozay, J. Scruggs, R. Vasudevan, and G. Orosz, “Connected and automated road vehicles: state of the art and future challenges,” *Vehicle system dynamics*, vol. 58, no. 5, pp. 672–704, 2020.

- [3] C. Fritschy and S. Spinler, “The impact of autonomous trucks on business models in the automotive and logistics industry—a delphi-based scenario study,” *Technological Forecasting and Social Change*, vol. 148, p. 119736, 2019.
- [4] M. Ben-Daya, E. Hassini, and Z. Bahroun, “Internet of things and supply chain management: a literature review,” *International Journal of Production Research*, vol. 57, no. 15-16, pp. 4719–4742, 2019.
- [5] A. Alam, B. Besselink, V. Turri, J. Mårtensson, and K. H. Johansson, “Heavy-duty vehicle platooning for sustainable freight transportation: A cooperative method to enhance safety and efficiency,” *IEEE Control Systems Magazine*, vol. 35, no. 6, pp. 34–56, 2015.
- [6] A. C. Manav and I. Lazoglu, “A novel cascade path planning algorithm for autonomous truck-trailer parking,” *IEEE Transactions on Intelligent Transportation Systems*, 2021.
- [7] J. Yuan, “Hierarchical motion planning for multisteering tractor-trailer mobile robots with on-axle hitching,” *IEEE/ASME Transactions on Mechatronics*, vol. 22, no. 4, pp. 1652–1662, 2017.
- [8] O. Ljungqvist, N. Evestedt, D. Axehill, M. Cirillo, and H. Pettersson, “A path planning and path-following control framework for a general 2-trailer with a car-like tractor,” *Journal of field robotics*, vol. 36, no. 8, pp. 1345–1377, 2019.
- [9] J. Jing, J. M. Maroli, Y. B. Salamah, M. Hejase, L. Fiorentini, and Ü. Özgüner, “Control method designs and comparisons for tractor-trailer vehicle backward path tracking,” in *2019 American Control Conference (ACC)*. IEEE, 2019, pp. 5531–5537.
- [10] Y. Sklyarenko, F. Schreiber, and W. Schumacher, “Maneuvering assistant for truck and trailer combinations with arbitrary trailer hitching,” in *2013 IEEE International Conference on Mechatronics (ICM)*. IEEE, 2013, pp. 774–779.
- [11] P. F. Lima, M. Nilsson, M. Trincavelli, J. Mårtensson, and B. Wahlberg, “Spatial model predictive control for smooth and accurate steering of an autonomous truck,” *IEEE Transactions on Intelligent Vehicles*, vol. 2, no. 4, pp. 238–250, 2017.
- [12] Y. Wang, “Improved A-search guided tree construction for kinodynamic planning,” in *2019 IEEE Int. Conf. Robot. Autom. (ICRA)*. IEEE, 2019, pp. 5530–5536.
- [13] A. Festag, A. Hessler, R. Baldessari, L. Le, W. Zhang, and D. Westhoff, “Vehicle-to-vehicle and road-side sensor communication for enhanced road safety,” in *World Congr. Intell. Transport Systems*, 2008.
- [14] D. Dolgov, S. Thrun, M. Montemerlo, and J. Diebel, “Practical search techniques in path planning for autonomous driving,” in *Proc. of the First International Symposium on Search Techniques in Artificial Intelligence and Robotics*, 2008.
- [15] H. J. Sussmann and G. Tang, “Shortest paths for the reeds-shepp car: a worked out example of the use of geometric techniques in nonlinear optimal control,” *Rutgers Center for Systems and Control Technical Report*, vol. 10, pp. 1–71, 1991.
- [16] M. Morari and U. Maeder, “Nonlinear offset-free model predictive control,” *Automatica*, vol. 48, no. 9, pp. 2059–2067, 2012.
- [17] S. Di Cairano and I. V. Kolmanovsky, “Real-time optimization and model predictive control for aerospace and automotive applications,” in *Amer. Control Conf.*, 2018, pp. 2392–2409.
- [18] S. Gros, M. Zanon, R. Quirynen, A. Bemporad, and M. Diehl, “From linear to nonlinear MPC: bridging the gap via the real-time iteration,” *International Journal of Control*, vol. 93, no. 1, pp. 62–80, 2020.
- [19] J. A. Andersson, J. Gillis, G. Horn, J. B. Rawlings, and M. Diehl, “CasADI: a software framework for nonlinear optimization and optimal control,” *Math. Program. Comput.*, vol. 11, no. 1, pp. 1–36, 2019.
- [20] R. Quirynen and S. Di Cairano, “PRESAS: Block-structured preconditioning of iterative solvers within a primal active-set method for fast model predictive control,” *Optimal Control Applications and Methods*, vol. 41, no. 6, pp. 2282–2307, 2020.
- [21] S. Dai and Y. Wang, “Long-horizon motion planning for autonomous vehicle parking incorporating incomplete map information,” in *2021 IEEE Int. Conf. Robot. Autom. (ICRA)*, 2021, pp. 8135–8142.
- [22] R. Quirynen, K. Berntorp, K. Kambam, and S. Di Cairano, “Integrated obstacle detection and avoidance in motion planning and predictive control of autonomous vehicles,” in *Proc. Am. Contr. Conf.*, 2020, pp. 1203–1208.